Hindawi Publishing Corporation
International Journal of Antennas and Propagation
Volume 2016, Article ID 8459109, 8 pages
http://dx.doi.org/10.1155/2016/8459109

Research Article

Design and Performance Analysis of MISO-ORM-DCSK System over Rayleigh Fading Channels

Gang Zhang,[1] Chuan gang Wang,[1] Guo quan Li,[2] and Jin zhao Lin[2]

[1] *Chongqing Key Laboratory of Signal and Information Processing, Chongqing University of Posts and Telecommunications, Chongqing 400065, China*
[2] *Chongqing Key Laboratory of Photoelectronic Information Sensing and Transmitting Technology, Chongqing University of Posts and Telecommunications, Chongqing 400065, China*

Correspondence should be addressed to Chuan gang Wang; 332694781@qq.com

Received 25 June 2016; Revised 4 September 2016; Accepted 4 October 2016

Academic Editor: Massimiliano Simeoni

A novel chaotic communication system, named Orthogonality-based Reference Modulated-Differential Chaos Shift Keying (ORM-DCSK), is proposed to enhance the performance of RM-DCSK. By designing an orthogonal chaotic generator (OCG), the intrasignal interference components in RM-DCSK are eliminated. Also, the signal frame format is expanded so the average bit energy is reduced. As a result, the proposed system has less interference in decision variables. Furthermore, to investigate the bit error rate (BER) performance over Rayleigh fading channels, the MISO-ORM-DCSK is studied. The BER expressions of the new system are derived and analyzed over AWGN channel and multipath Rayleigh fading channel. All simulation results not only show that the proposed system can obtain significant improvement but also verify the analysis in theory.

1. Introduction

Chaos based digital communication systems have been proposed and studied in recent years [1–7]. The differential chaos shift keying (DCSK) and its constant power version called frequency-modulated DCSK (FM-DCSK) are widely studied. However, the drawbacks of DCSK or FM-DCSK are low data rate and poor security [1, 2]. In order to address those problems, NR-DCSK, OFDM-DCSK, and short reference DCSK are proposed in [8–10]. Based on the robustness of DCSK against linear and nonlinear channel distortions, Kaddoum et al. studied DCSK for PLC applications. On the other hand, smart antenna technology can eliminate the multipath wave propagation [11]. Therefore, MIMO-DCSK and STBC-DCSK are proposed to improve the performance of DCSK system [12–14]. Furthermore, the reference modulated DCSK (RM-DCSK) is proposed in [15]. In RM-DCSK system, the chaotic signal sent in each time slot not only carries one bit of information but also serves as the reference signal of the information bit transmitted in its following slot. For this reason, the attainable data rate of RM-DCSK is doubled in comparison to DCSK. However, the intrasignal interference is produced in decision variables at the receiver. Therefore, compared to DCSK, BER performance of RM-DCSK is not improved.

In this paper, the ORM-DCSK system is proposed as an improved version for RM-DCSK. A novel orthogonal chaotic generator (OCG) is designed to generate orthogonal chaos signal. Also, the signal frame format is extended. Furthermore, two transmit antennas are used in the transmitter of the ORM-DCSK and BER formula is derived.

The remainder of this paper is organized as follows: in Section 2, the principle of MISO-ORM-DCSK is presented. In Section 3, the BER expressions are analyzed. In Section 4, simulation results are shown to evaluate the performance of the new system. Finally, summaries are given in Section 5.

2. MISO-ORM-DCSK

In this section, the baseband implementation of MISO-ORM-DCSK is introduced and some details are explained.

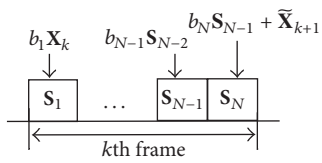

Figure 1: Signal frame format of ORM-DCSK.

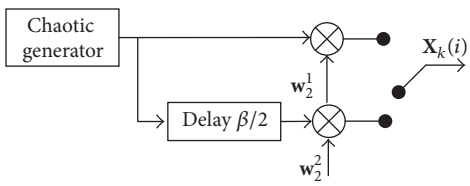

Figure 2: Block diagram of OCG.

2.1. Signal Format. Figure 1 shows the frame format of ORM-DCSK system. Different with RM-DCSK, there are N adjacent time slots in each frame, in which average bit energy (labeled as E_b) decreases from $1.5\beta E(x_i^2)$ to $(1+1/N)\beta E(x_i^2)$. The time slot is divided into β chips to carry the chaotic sequences and b_l is the lth information bit in kth frame. Concretely, $\mathbf{X}_k$ is modulated by the information bit $b_1 \in \{+1,-1\}$ in the first time slot of kth frame. In the second time slot, $b_2 b_1 \mathbf{X}_k$ is sent. In the Nth time slot, $b_N \cdots b_1 \mathbf{X}_k + \widetilde{\mathbf{X}}_{k+1}$ is sent. Here, $\widetilde{\mathbf{X}}_{k+1}$ can be converted into the reference sequence of $(k+1)$th frame. In Figure 1, $\mathbf{X}_k = (1/\sqrt{M_T}) \cdot [x_k(1), x_k(2), \ldots, x_k(\beta)]$ and M_T is the number of transmit antennas.

2.2. Transmitter Structure. Figure 2 shows the block diagram of orthogonal chaotic generator (OCG). It is necessary to make the chaotic carriers transmitted in neighboring two frames orthogonal to erase the intrasignal interference components included in decision variables clearly. We assume that the spreading factor is six ($\beta = 6$). In the first-time slot period, as shown in Figure 2, the switch is connected to bottom. The chaotic sequence $\mathbf{U} = [a, b, c]$ is multiplied by $\mathbf{w}_2^2 = [+1, -1]$. In other words, $\mathbf{X}_k = \mathbf{U} \cdot \mathbf{w}_2^2 = [a, -a, b, -b, c, -c]$. During second- to $(N-1)$th-slots period, the switch is suspended. In the Nth-time slot period, the switch is connected to bottom. The chaotic sequence $\mathbf{V} = [x, y, z]$ is multiplied by $\mathbf{w}_2^1 = [+1, +1]$. $\widetilde{\mathbf{X}}_{k+1} = \mathbf{V} \cdot \mathbf{w}_2^1 = [x, x, y, y, z, z]$. In the first-time slot period of $(k+1)$th frame, the switch is connected to bottom again. $\mathbf{X}_{k+1} = \mathbf{V} \cdot \mathbf{w}_2^2 = [x, -x, y, -y, z, -z]$.

The chaotic sequences generated by the OCG satisfy

$$\begin{aligned} &\mathbf{X}_k \perp \widetilde{\mathbf{X}}_{k+1}, \\ &\widetilde{\mathbf{X}}_{k+1} \perp \mathbf{X}_{k+1}, \\ &\mathbf{X}_{k+1} = \left(\widetilde{\mathbf{X}}_{k+1}\mathbf{W}\right), \\ &\mathbf{X}_{k+1} \perp \left(\mathbf{X}_k\mathbf{W}\right). \end{aligned} \tag{1}$$

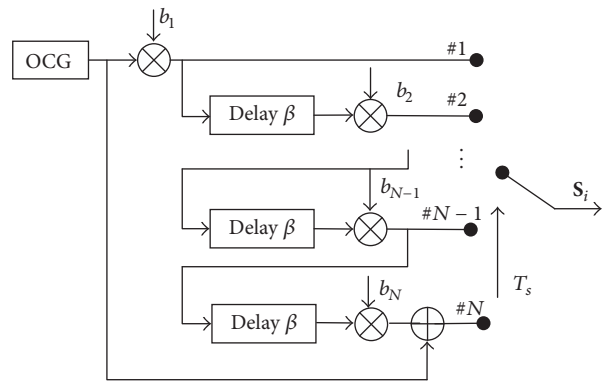

Figure 3: Block diagram of the proposed system transmitter.

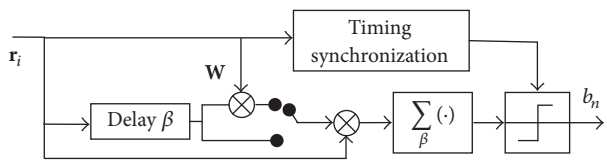

Figure 4: Block diagram of the proposed system receiver.

Here $\mathbf{W} = \underbrace{[+1, -1 \cdots +1, -1]}_{\beta}$ is a modification function.

Figure 3 shows the block diagram of ORM-DCSK transmitter. There are two transmitting antennas ($M_T = 2$) and one receiving antenna in MISO-ORM-DCSK system. The two transmitting antennas are independent. The signal can be sent by number 1 antenna and the replica of the signal can be sent by number 2 antenna. The transmit signal and replica can be sent at the same time in theory. However, it may be hardly implementable at present due to plenty of delay lines in transmitter. To replace the delay circuit, some excellent algorithms could be employed here, which are provided in [16]. As described in Figure 1, the transmitted signal in kth frame is denoted by

$$\begin{aligned} &\mathbf{S}_1 = b_1\mathbf{X}_k, \\ &\mathbf{S}_l = b_l\mathbf{S}_{l-1} \quad (l = 2, \ldots, N-1), \\ &\mathbf{S}_N = b_N\mathbf{S}_{N-1} + \widetilde{\mathbf{X}}_{k+1}. \end{aligned} \tag{2}$$

2.3. Receiver Structure. The receiver structure of ORM-DCSK is depicted in Figure 4, which has similar appearance to RM-DCSK detector. In our receiver, to demodulate b_1, we make the switch up. The modification function $\mathbf{W}$ is used to adjust the relationship between signal in first bit period of kth frame and signal in its former time slot. When decoding b_l ($l = 2, 3, \ldots, N$) of kth frame, we make the switch down. Furthermore, the information extraction could work quite well if the receiver knows the starting time of each time slot. As a result, there is a timing synchronization circuit in our receiver, as done in RM-DCSK. To acquire perfect bit synchronization, many traditional timing techniques could be adopted, like data-aided timing synchronization algorithm designed for DCSK [17].

2.4. Channel Model. The channel between each transmit antenna and the receive antenna is two-ray Rayleigh quasi-static block faded channel. $\boldsymbol{\xi}$ denotes a noise sample following a Gaussian distribution with zero mean and variance $N_0/2$. Further, $\alpha_{m,1}$ and $\alpha_{m,2}$ denote the gains of the two paths between mth ($m = 1, 2$) transmit antenna and the receive antenna, which are independent, Rayleigh distributed random variables. It is assumed that the channel state remains constant during each bit period.

According to different channel gains, we consider the following two cases:

$$\begin{aligned} &\text{Case 1: } E\left\{(\alpha_1)^2\right\} = E\left\{(\alpha_2)^2\right\} = \frac{1}{2}, \\ &\text{Case 2: } E\left\{(\alpha_1)^2\right\} = \frac{2}{3}, \\ &\qquad\qquad E\left\{(\alpha_2)^2\right\} = \frac{1}{3} \end{aligned} \tag{3}$$

At the receiver, we denote the received signal vector during the bit duration by $\mathbf{r}_l$ ($l = 1, \ldots, N$). Then, $\mathbf{r}_l$ can be given by

$$\mathbf{r}_l = \sum_{m=1}^{M_T} \alpha_{m,1} \mathbf{s}_{m,l}^{\tau_{m,1}} + \sum_{m=1}^{M_T} \alpha_{m,2} \mathbf{s}_{m,l}^{\tau_{m,2}} + \boldsymbol{\xi}_l. \tag{4}$$

Here, $\mathbf{s}_{m,l}^{\tau_{m,i}}$ ($i = 1, 2$) is delayed signal transmitted during lth bit duration and $\boldsymbol{\xi}_l$ is the additive white Gaussian noise vector.

As described in Figure 1, the chaotic wavelet sent in each time slot not only carries one bit of data but also serves as the reference signal of the data bit transmitted in its next time slot. Then, $\mathbf{r}_{l-1}$ can be denoted as the reference segment for $\mathbf{r}_l$. In this case, the outputs of the demodulators should be given by

$$\begin{aligned} c_1 &= \mathbf{r}_1 \cdot \mathbf{r}_0 \cdot \mathbf{w}, \\ c_l &= \mathbf{r}_l \cdot \mathbf{r}_{l-1} \quad (l = 2, \ldots, N). \end{aligned} \tag{5}$$

In (5), $\mathbf{r}_0$ is signal of last slot time of previews frame.

Finally, based on the following rule, the estimated information bit is decided as "+1" or "−1":

$$\hat{b}_l = \begin{cases} +1, & c_i > 0, \\ -1, & c_i < 0. \end{cases} \tag{6}$$

3. Performance Analysis

In this section, BER expression is derived over Rayleigh fading channels. Based on Figure 1 and (5), it can be easily found that the statistical properties of c_l ($l = 1, 2, \ldots, N$) are different. Then, we must calculate the BER performance of each bit, which differs from RM-DCSK.

The logistic map $x_{i+1} = 1 - 2x_i^2$, $-1 < x_i < 1$, $x_i \neq \{0, \pm 0.5\}$, is used with $E(x_i) = 0$ and $E(x_i^2) = 0.5$, $\mathrm{Var}(x_i^2) = 0.125$, where $E(\cdot)$and $\mathrm{Var}(\cdot)$ denote the expectation operator and variance operator, respectively. We can get the average bit energy $E_b = (1 + 1/N)\beta E(x_i^2)$.

To further simplify the analysis, we can assume that $\tau_{m,1} = 0$, $\tau_{m,2} = \tau$, and multipath time delay is much smaller than the spreading factor; that is, $0 < \tau \ll \beta$. Thus, (4) can be rewritten as

$$\mathbf{r}_l = \sum_{m=1}^{M_T} \alpha_{m,1} \mathbf{s}_{m,l} + \sum_{m=1}^{M_T} \alpha_{m,2} \mathbf{s}_{m,l}^{\tau} + \boldsymbol{\xi}_l \tag{7}$$

Therefore, without loss of generality, we consider the error rate of the bit b_2. Substituting (7) into (5) for $l = 2$, we can get

$$\begin{aligned} c_2 &= \mathbf{r}_2 \cdot \mathbf{r}_1 \\ &= \left[\frac{1}{\sqrt{M_T}} \left(b_2 b_1 \mathbf{X}_k \sum_{m=1}^{M_T} \alpha_{m,1} + b_2 b_1 \mathbf{X}_k^{\tau} \sum_{m=1}^{M_T} \alpha_{m,2} \right) + \boldsymbol{\xi}_2 \right] \\ &\quad \cdot \left[\frac{1}{\sqrt{M_T}} \left(b_1 \mathbf{X}_k \sum_{m=1}^{M_T} \alpha_{m,1} + b_1 \mathbf{X}_k^{\tau} \sum_{m=1}^{M_T} \alpha_{m,2} \right) + \boldsymbol{\xi}_1 \right] \\ &= \mathrm{A} + \mathrm{B} + \underbrace{\boldsymbol{\xi}_1 \cdot \boldsymbol{\xi}_2}_{\mathrm{C}}, \end{aligned} \tag{8}$$

where

$$\begin{aligned} \mathrm{A} &= \frac{1}{M_T} \left(b_2 b_1 \mathbf{X}_k \sum_{m=1}^{M_T} \alpha_{m,1} + b_2 b_1 \mathbf{X}_k^{\tau} \sum_{m=1}^{M_T} \alpha_{m,2} \right) \\ &\quad \cdot \left(b_1 \mathbf{X}_k \sum_{m=1}^{M_T} \alpha_{m,1} + b_1 \mathbf{X}_k^{\tau} \sum_{m=1}^{M_T} \alpha_{m,2} \right), \\ \mathrm{B} &= \frac{1}{\sqrt{M_T}} \left(b_2 b_1 \mathbf{X}_k \sum_{m=1}^{M_T} \alpha_{m,1} + b_2 b_1 \mathbf{X}_k^{\tau} \sum_{m=1}^{M_T} \alpha_{m,2} \right) \boldsymbol{\xi}_1 \\ &\quad + \frac{1}{\sqrt{M_T}} \left(b_1 \mathbf{X}_k \sum_{m=1}^{M_T} \alpha_{m,1} + b_1 \mathbf{X}_k^{\tau} \sum_{m=1}^{M_T} \alpha_{m,2} \right) \boldsymbol{\xi}_2. \end{aligned} \tag{9}$$

Assuming $b_2 = 1$, the instantaneous mean of the decision variable is $E(c_2) = E(\mathrm{A}) + E(\mathrm{B}) + E(\mathrm{C})$. Here,

$$\begin{aligned} E(\mathrm{A}) &= \left[\left(\sum_{m=1}^{M_T} \alpha_{m,1} \right)^2 + \left(\sum_{m=1}^{M_T} \alpha_{m,2} \right)^2 \right] \frac{N E_b}{(N+1) M_T}, \\ E(\mathrm{B}) &= E(\mathrm{C}) = 0. \end{aligned} \tag{10}$$

The variance of decision variable can be easily expressed as $\mathrm{Var}(c_2) = \mathrm{Var}(\mathrm{A}) + \mathrm{Var}(\mathrm{B}) + \mathrm{Var}(\mathrm{C})$. Here,

$$\begin{aligned} \mathrm{Var}(\mathrm{A}) &= \frac{\beta \left[\left(\sum_{m=1}^{M_T} \alpha_{m,1} \right)^4 + \left(\sum_{m=1}^{M_T} \alpha_{m,2} \right)^4 \right]}{8 M_T^2} \\ &\quad + \frac{2 \left(\sum_{m=1}^{M_T} \alpha_{m,1} \right)^2 \left(\sum_{m=1}^{M_T} \alpha_{m,2} \right)^2 N^2 E_b^2}{\beta (N+1)^2 M_T^2} \end{aligned}$$

$$\begin{aligned}\mathrm{Var}(\mathrm{B}) &= \frac{\left[\left(\sum_{m=1}^{M_T}\alpha_{m,1}\right)^2+\left(\sum_{m=1}^{M_T}\alpha_{m,2}\right)^2\right]NE_bN_0}{(N+1)M_T}\\ \mathrm{Var}(\mathrm{C}) &= \beta\frac{N_0^2}{4}.\end{aligned} \tag{11}$$

Based on the above results, the mean and variance of c_2 are

$$\begin{aligned}&E(c_2 \mid b_2=+1)\\ &\quad=\left[\left(\sum_{m=1}^{M_T}\alpha_{m,1}\right)^2+\left(\sum_{m=1}^{M_T}\alpha_{m,2}\right)^2\right]\frac{NE_b}{(N+1)M_T}.\\ &\mathrm{Var}(c_2 \mid b_2=+1)\\ &\quad=\frac{\beta\left[\left(\sum_{m=1}^{M_T}\alpha_{m,1}\right)^4+\left(\sum_{m=1}^{M_T}\alpha_{m,2}\right)^4\right]}{8M_T^2}\\ &\qquad+\frac{2\left(\sum_{m=1}^{M_T}\alpha_{m,1}\right)^2\left(\sum_{m=1}^{M_T}\alpha_{m,2}\right)^2N^2E_b^2}{\beta(N+1)^2M_T^2}\\ &\qquad+\frac{\left[\left(\sum_{m=1}^{M_T}\alpha_{m,1}\right)^2+\left(\sum_{m=1}^{M_T}\alpha_{m,2}\right)^2\right]NE_bN_0}{(N+1)M_T}\\ &\qquad+\beta\frac{N_0}{4}\end{aligned} \tag{12}$$

Similarly, if $b_2=-1$ is sent, the mean and variance of c_2 are equal to

$$\begin{aligned}E(c_2 \mid b_2=-1) &= -E(c_2 \mid b_2=+1)\\ \mathrm{Var}(c_2 \mid b_2=-1) &= \mathrm{Var}(c_2 \mid b_2=+1).\end{aligned} \tag{13}$$

Based on the above results, the BER for decoding b_l is computed as

$$\begin{aligned}\mathrm{BER}_{c_2}(\gamma_b) &= \frac{1}{2}\mathrm{erfc}\left[\frac{E(c_2 \mid b_2=+1)}{\sqrt{2\,\mathrm{Var}(c_2 \mid b_2=+1)}}\right]\\ &= \frac{1}{2}\mathrm{erfc}\left[\left(\frac{\Lambda_1}{\beta}+\frac{2\Gamma}{\gamma_b}+\frac{\beta\Gamma^2}{2\gamma_b^2}\right)^{-1/2}\right].\end{aligned} \tag{14}$$

Similarly, for $l\in\{3,4,\ldots,N-1\}$ the BER is

$$\mathrm{BER}_{c_l}(\gamma_b)=\mathrm{BER}_{c_2}(\gamma_b). \tag{15}$$

For $l=1$, we can get

$$\begin{aligned}c_1 &= \mathbf{r}_1\cdot\mathbf{r}_0\cdot\mathbf{w}=\left[\frac{1}{\sqrt{M_T}}\left(b_1\mathbf{X}_k\sum_{m=1}^{M_T}\alpha_{m,1}\right.\right.\\ &\quad\left.\left.+b_1\mathbf{X}_k^{\tau}\sum_{m=1}^{M_T}\alpha_{m,2}\right)+\boldsymbol{\xi}_1\right]\\ &\quad\cdot\left[\frac{1}{\sqrt{M_T}}\left(\left(b_0\mathbf{X}_{k-1}+\widetilde{\mathbf{X}}_k\right)\mathbf{w}\sum_{m=1}^{M_T}\alpha_{m,1}\right.\right.\\ &\quad\left.\left.+\left(b_0\mathbf{X}_{k-1}^{\tau}+\widetilde{\mathbf{X}}_k^{\tau}\right)\mathbf{w}^{\tau}\sum_{m=1}^{M_T}\alpha_{m,2}\right)+\boldsymbol{\xi}_0\mathbf{w}\right]=\mathrm{D}+\mathrm{E}\\ &\quad+\underbrace{\boldsymbol{\xi}_1\cdot\boldsymbol{\xi}_0\mathbf{w}}_{\mathrm{F}},\end{aligned} \tag{16}$$

where

$$\begin{aligned}\mathrm{D} &= \frac{1}{M_T}\left(b_1\mathbf{X}_k\sum_{m=1}^{M_T}\alpha_{m,1}+b_1\mathbf{X}_k^{\tau}\sum_{m=1}^{M_T}\alpha_{m,2}\right)\\ &\quad\cdot\left[\left(b_0\mathbf{X}_{k-1}\mathbf{w}+\mathbf{X}_k\right)\sum_{m=1}^{M_T}\alpha_{m,1}\right.\\ &\quad\left.+\left(b_0\mathbf{X}_{k-1}^{\tau}\mathbf{w}^{\tau}+\mathbf{X}_k^{\tau}\right)\sum_{m=1}^{M_T}\alpha_{m,2}\right],\\ \mathrm{E} &= \frac{1}{\sqrt{M_T}}\left(b_1\mathbf{X}_k\sum_{m=1}^{M_T}\alpha_{m,1}+b_1\mathbf{X}_k^{\tau}\sum_{m=1}^{M_T}\alpha_{m,2}\right)\boldsymbol{\xi}_0\mathbf{w}\\ &\quad+\frac{1}{\sqrt{M_T}}\left[\left(b_0\mathbf{X}_{k-1}\mathbf{w}+\mathbf{X}_k\right)\sum_{m=1}^{M_T}\alpha_{m,1}\right.\\ &\quad\left.+\left(b_0\mathbf{X}_{k-1}^{\tau}\mathbf{w}^{\tau}+\mathbf{X}_k^{\tau}\right)\sum_{m=1}^{M_T}\alpha_{m,2}\right]\boldsymbol{\xi}_1.\end{aligned} \tag{17}$$

Similarly, we can get

$$E(\mathrm{D})=\left[\left(\sum_{m=1}^{M_T}\alpha_{m,1}\right)^2+\left(\sum_{m=1}^{M_T}\alpha_{m,2}\right)^2\right]\frac{NE_b}{(N+1)M_T}, \tag{18}$$

$$E(\mathrm{E})=E(\mathrm{F})=0, \tag{19}$$

$$\begin{aligned}&\mathrm{Var}(\mathrm{D})\\ &\quad=\frac{\beta\left[\left(\sum_{m=1}^{M_T}\alpha_{m,1}\right)^4+\left(\sum_{m=1}^{M_T}\alpha_{m,2}\right)^4\right]}{8M_T^2}\\ &\qquad+\frac{4\left(\sum_{m=1}^{M_T}\alpha_{m,1}\right)^2\left(\sum_{m=1}^{M_T}\alpha_{m,2}\right)^2N^2E_b^2}{\beta(N+1)^2M_T^2},\end{aligned} \tag{20}$$

$$\mathrm{Var}\,(\mathrm{E}) = \frac{3\left[\left(\sum_{m=1}^{M_T}\alpha_{m,1}\right)^2 + \left(\sum_{m=1}^{M_T}\alpha_{m,2}\right)^2\right]NE_bN_0}{2\,(N+1)\,M_T}, \tag{21}$$

$$\mathrm{Var}\,(\mathrm{F}) = \beta\frac{N_0^2}{4}. \tag{22}$$

So, the mean and variance of c_1 are

$$\begin{aligned} &E\left(c_1 \mid b_1 = +1\right) \\ &\quad = \left[\left(\sum_{m=1}^{M_T}\alpha_{m,1}\right)^2 + \left(\sum_{m=1}^{M_T}\alpha_{m,2}\right)^2\right]\frac{NE_b}{(N+1)\,M_T}, \end{aligned} \tag{23}$$

$$\begin{aligned} &\mathrm{Var}\left(c_1 \mid b_1 = +1\right) \\ &\quad = \frac{\beta\left[\left(\sum_{m=1}^{M_T}\alpha_{m,1}\right)^4 + \left(\sum_{m=1}^{M_T}\alpha_{m,2}\right)^4\right]}{8M_T^2} \\ &\qquad + \frac{4\left(\sum_{m=1}^{M_T}\alpha_{m,1}\right)^2\left(\sum_{m=1}^{M_T}\alpha_{m,2}\right)^2 N^2E_b^2}{\beta\,(N+1)^2\,M_T^2} \\ &\qquad + \frac{3NE_bN_0\left[\left(\sum_{m=1}^{M_T}\alpha_{m,1}\right)^2 + \left(\sum_{m=1}^{M_T}\alpha_{m,2}\right)^2\right]}{2\,(N+1)\,M_T} \\ &\qquad + \beta\frac{N_0}{4}. \end{aligned} \tag{24}$$

Based on (23)-(24), the BER for decoding b_1 is computed as

$$\begin{aligned} \mathrm{BER}_{c_1}\left(\gamma_b\right) &= \frac{1}{2}\mathrm{erfc}\left[\frac{E\left(c_1 \mid b_1 = +1\right)}{\sqrt{2\mathrm{Var}\left(c_1 \mid b_1 = +1\right)}}\right] \\ &= \frac{1}{2}\mathrm{erfc}\left[\left(\frac{\Lambda_2}{\beta} + \frac{3\Gamma}{\gamma_b} + \frac{\beta\Gamma^2}{2\gamma_b^2}\right)^{-1/2}\right]. \end{aligned} \tag{25}$$

Here,

$$\begin{aligned} \Lambda_1 &= 1 + \frac{2\left(\sum_{m=1}^{M_T}\alpha_{m,1}\sum_{m=1}^{M_T}\alpha_{m,2}\right)^2}{\left(\left(\sum_{m=1}^{M_T}\alpha_{m,1}\right)^2 + \left(\sum_{m=1}^{M_T}\alpha_{m,2}\right)^2\right)^2}, \\ \Lambda_2 &= 1 + \frac{6\left(\sum_{m=1}^{M_T}\alpha_{m,1}\sum_{m=1}^{M_T}\alpha_{m,2}\right)^2}{\left(\left(\sum_{m=1}^{M_T}\alpha_{m,1}\right)^2 + \left(\sum_{m=1}^{M_T}\alpha_{m,2}\right)^2\right)^2}, \\ \Gamma &= 1 + \frac{1}{N} \\ \gamma_b &= \underbrace{\frac{\left(\sum_{m=1}^{M_T}\alpha_{m,1}\right)^2 E_b}{M_TN_0}}_{\overline{\gamma_1}} + \underbrace{\frac{\left(\sum_{m=1}^{M_T}\alpha_{m,2}\right)^2 E_b}{M_TN_0}}_{\overline{\gamma_2}}. \end{aligned} \tag{26}$$

We denote $\overline{\gamma_1} = E(\gamma_1)$ and $\overline{\gamma_2} = E(\gamma_2)$ to represent the average SNR per path. Moreover, for a multipath Rayleigh fading channel, the PDF of γ_b is given by

$$f\left(\gamma_b\right) = \begin{cases} \dfrac{\gamma_b}{\overline{\gamma_1}^2}e^{-\gamma_b/\overline{\gamma_1}}, & E\left(\alpha_1^2\right) = E\left(\alpha_2^2\right), \\ \dfrac{e^{-\gamma_b/\overline{\gamma_1}} - e^{-\gamma_b/\overline{\gamma_2}}}{\overline{\gamma_1} - \overline{\gamma_2}}, & E\left(\alpha_1^2\right) \neq E\left(\alpha_2^2\right). \end{cases} \tag{27}$$

Based on (14)–(16), the BER is

$$\begin{aligned} \mathrm{BER}\left(\gamma_b\right) &= \frac{N-2}{2N}\mathrm{erfc}\left[\left(\frac{\Lambda_1}{\beta} + \frac{2\Gamma}{\gamma_b} + \frac{\beta\Gamma^2}{2\gamma_b^2}\right)^{-1/2}\right] \\ &\quad + \frac{1}{N}\mathrm{erfc}\left[\left(\frac{\Lambda_2}{\beta} + \frac{3\Gamma}{\gamma_b} + \frac{\beta\Gamma^2}{2\gamma_b^2}\right)^{-1/2}\right]. \end{aligned} \tag{28}$$

Finally, using (20) and (21), the BER of MISO-ORM-DCSK is derived as

$$\mathrm{BER} = \int_0^\infty \mathrm{BER}\left(\gamma_b\right) f\left(\gamma_b\right) d\gamma_b. \tag{29}$$

Moreover, we can get the theoretical lower bound of the BER when N tends to infinity.

$$\begin{aligned} \mathrm{BER}_{\mathrm{lowerBound}}\left(\gamma_b\right) &= \lim_{N\to\infty}\mathrm{BER}\left(\gamma_b\right) \\ &= \frac{1}{2}\mathrm{erfc}\left\{\left[\frac{\Lambda_1}{\beta} + \frac{2}{\gamma_b} + \frac{\beta}{2\gamma_b^2}\right]^{-1/2}\right\}, \\ \mathrm{BER}_{\mathrm{lowerBound}} &= \int_0^\infty \mathrm{BER}_{\mathrm{lowerBound}}\left(\gamma_b\right) f\left(\gamma_b\right) d\gamma_b. \end{aligned} \tag{30}$$

On the other hand, (28) can be extended to the AWGN channel case by choosing $\alpha_{m,1} = 1$ and $\alpha_{m,2} = 0$. Hence, the BER would simplify to

$$\begin{aligned} \mathrm{BER} &= \frac{N-2}{2N}\mathrm{erfc}\left[\left(\frac{1}{\beta} + \frac{\Gamma N_0}{E_b} + \frac{\beta\Gamma^2N_0^2}{8E_b^2}\right)^{-1/2}\right] \\ &\quad + \frac{1}{N}\mathrm{erfc}\left[\left(\frac{1}{\beta} + \frac{3\Gamma N_0}{2E_b} + \frac{\beta\Gamma^2N_0^2}{8E_b^2}\right)^{-1/2}\right]. \end{aligned} \tag{31}$$

4. Simulation

In order to validate the BER performance of the MISO-ORM-DCSK and compare it with MISO-RM-DCSK, the BER is evaluated under AWGN and multipath fading channels. To facilitate the expression, the Monte Carlo simulations and theory results are labeled as "Sim" and "Theory" respectively.

4.1. AWGN Channel. Since the theoretical BERs for the 2nd to $(N-1)$th bits and the BER for Nth bit are different, Figure 5 shows BERs for $(N-1)$th bit and Nth bit in the AWGN channel of MISO-ORM-DCSK for $\beta = 256$ and $N = 4$.

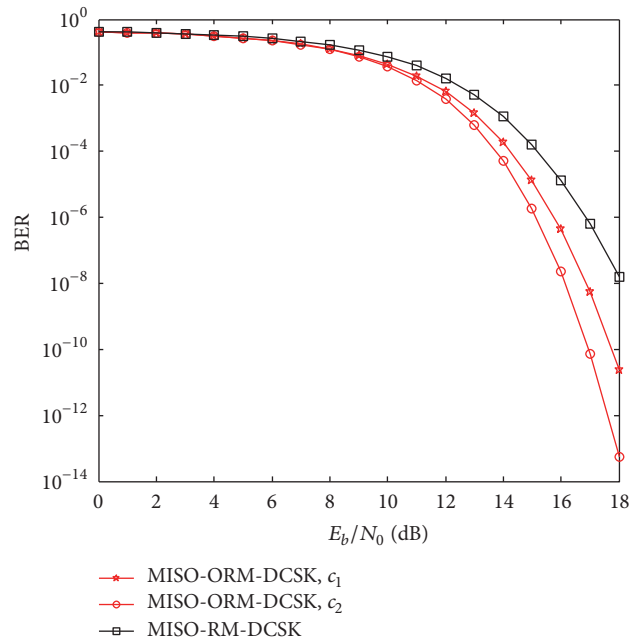

Figure 5: Each BER in the AWGN channel for MISO-ORM-DCSK.

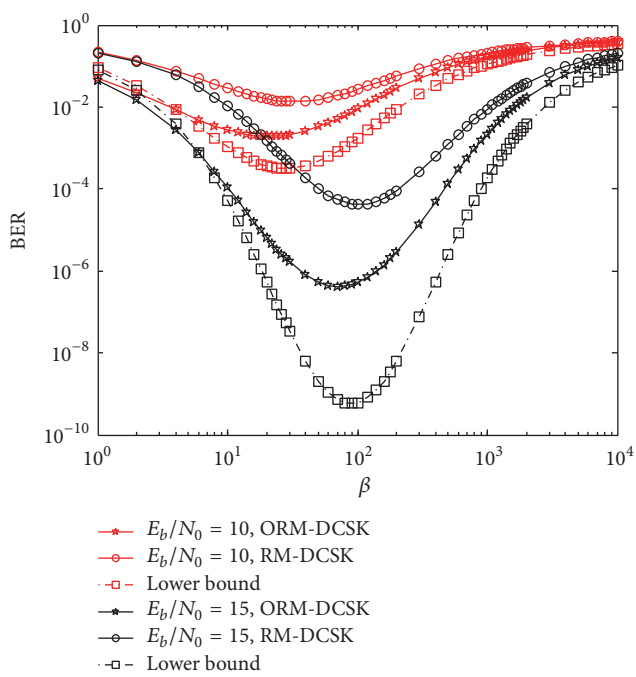

Figure 6: BER performance versus spreading factor β.

From Figure 5, it is shown that as E_b/N_0 increases, the BERs become better. In addition, the error rate of c_2 is superior to that of c_1 in the proposed system. This can be explained as follows: the decision variable of c_1 has an interference term, which does not exist in that of c_2. It is visible that, with less intrasignal interference and noise interference components, MISO-ORM-DCSK is always better than MISO-RM-DCSK.

Figure 6 shows the relationship between BER performance and spreading factor β. It can also be noticed that

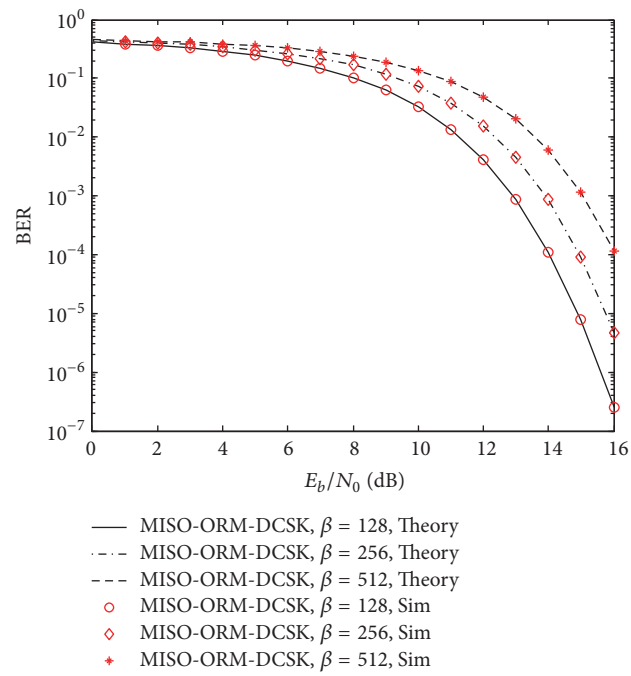

Figure 7: Relationships between analytical BER and Monte Carlo results for MISO-ORM-DCSK and MISO-RM-DCSK with $N = 2$.

ORM-DCSK is always better than RM-DCSK. In addition, it is obvious that the BER can maximize an optimal value by choosing the certain value of spreading factor; for example, the certain value is about 30 and 100 when $E_b/N_0 = 10$ dB and $E_b/N_0 = 15$ dB, respectively. BER starts to degrade if the spreading factor is beyond it, which is caused by fluctuations in E_b at small β and the noise-noise cross correlation at large β.

Figure 7 shows the relationships between analytical BER and Monte Carlo of MISO-ORM-DCSK in the AWGN channel. From Figure 7, it is easily found that clear matching between analytical expression and Monte Carlo simulations result can be obtained. This confirms that the Gaussian approximation works well when the spreading factor is relatively lager.

Figure 8 plots the relationships between BER performance and N with $E_b/N_0 = 18$ dB and $\beta = 256$. The BER is smaller with larger N. We can get the theoretical lower bound of the BER when N tends to infinity. However, the complexity of system is increasing. We think $N \leq 50$ is the best choice and it can bring a trade-off between the BER and complexity.

4.2. Rayleigh Fading Channel. Figure 9 plots the relationships between BER performance and E_b/N_0 for MISO-ORM-DCSK and MISO-RM-DCSK system with $N = 4$. Through the examination of Figure 9, the proposed system achieves a performance gain of about 2 dB over the MISO-RM-DCSK at BER $= 1 \times 10^{-4}$. In other words, the new system shows an enhanced robustness in Rayleigh fading channel.

Figure 10 shows the relationships between analytical BER and Monte Carlo results in Rayleigh fading channel when spreading factors $\beta = 128$ and 512 and $N = 2$. It is easily

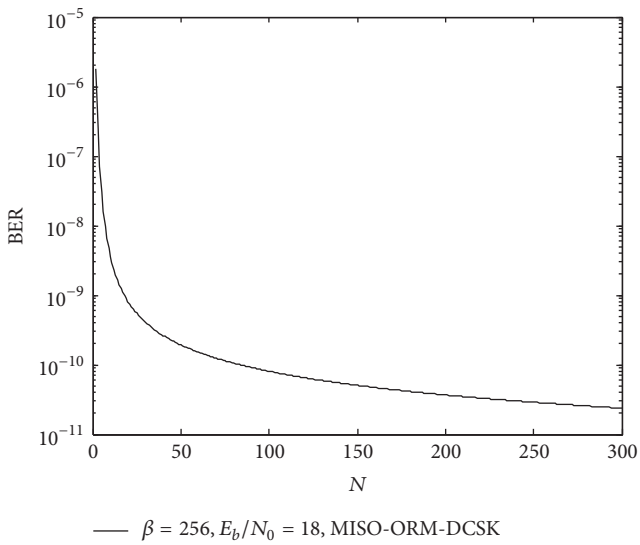

Figure 8: Relationships between BER and N for MISO-ORM-DCSK.

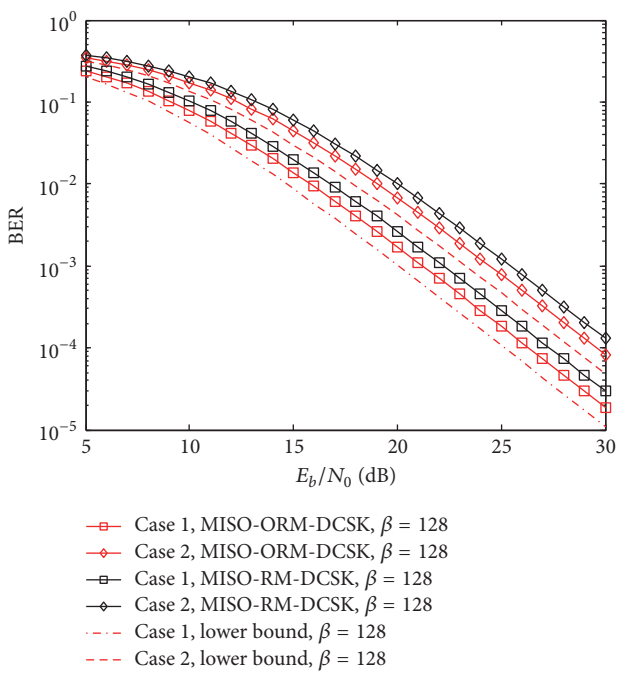

Figure 9: BER performance in Rayleigh fading channel with different gains.

found that analytical results correspond with simulation results perfectly. This can be explained by identical reason in Figure 7 and the Gaussian approximation works well when the spreading factor is relatively lager. In addition, the BERs for all cases become worse as β increases, which can be attributed to the increasing negative contribution from interference components generated from the chaotic sequence and Gaussian noise.

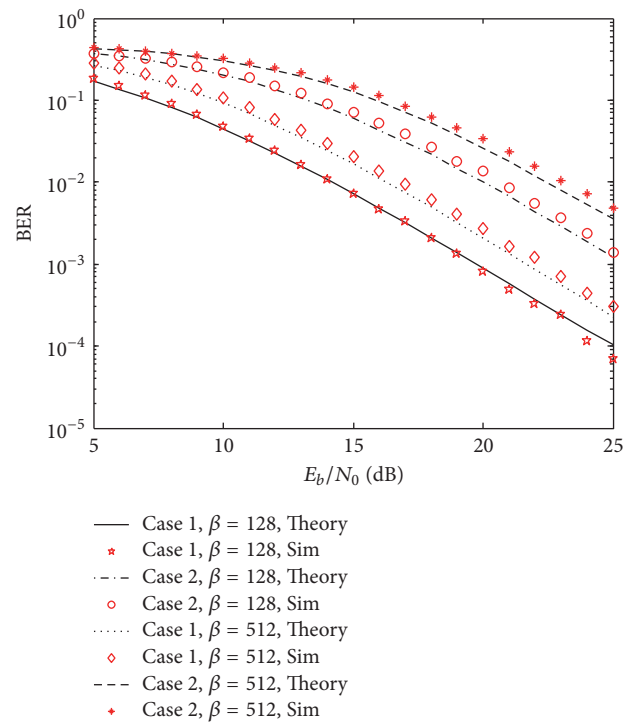

Figure 10: Relationships between analytical BER and Monte Carlo results in Rayleigh fading channel.

5. Conclusion

In this paper, ORM-DCSK is proposed to improve the BER performance of RM-DCSK. The intrasignal interference components existing in RM-DCSK are eliminated clearly by designing an orthogonal chaotic generator. Without any cost in data rate, the proposed system not only shows excellent agreement between theoretical expressions and Monte Carlo simulations but also shows significance of BER improvement.

However, the proposed system is slightly more complex than RM-DCSK due to additional delay and switch. This complexity cost is worthy and it provides a huge BER improvement. We believe that the proposed system has significant potential in chaotic communication environment.

Competing Interests

The authors declare that they have no competing interests.

Acknowledgments

This work was supported in part by the National Natural Science Foundation of China under Grants no. 61371164, no. 61301124, and no. 61671091 and in part by the Chongqing Distinguished Youth Foundation no. CSTC2011jjjq40002, as well as the University Innovation Team Construction Plan of Smart Medical System and Core Technology.

References

[1] G. Kolumban, B. Vizvari, W. Schwarz et al., "Differential chaos shift keying: a robust coding for chaos communications," in *Proceedings of the IEEE Workshop on Nonlinear Dynamics of Electronic Systems (NDES '96)*, pp. 87–92, Seville, Spain, 1996.

[2] G. Kolumban, G. Kis, M. P. Kennedy et al., "FM-DCSK: a new and robust solution to chaos communications," in *Proceedings of the International Symposium on Nonlinear Theory and Applications*, pp. 117–120, 1997.

[3] L. Wang, G. Cai, and G. R. Chen, "Design and performance analysis of a new multiresolution M-Ary differential chaos shift keying communication system," *IEEE Transactions on Wireless Communications*, vol. 14, no. 9, pp. 5197–5208, 2015.

[4] A. Kumar and P. R. Sahu, "Performance analysis of DCSK-SR systems based on best relay selection in multiple MIMO relay environment," *International Journal of Electronics and Communications*, vol. 70, no. 1, pp. 18–24, 2016.

[5] G. Kaddoum and F. Shokraneh, "Analog network coding for multi-user multi-carrier differential chaos shift keying communication system," *IEEE Transactions on Wireless Communications*, vol. 14, no. 3, pp. 1492–1505, 2015.

[6] Y. Fang, L. Wang, P. Chen, J. Xu, G. Chen, and W. Xu, "Design and analysis of a DCSK-ARQ/CARQ system over multipath fading channels," *IEEE Transactions on Circuits and Systems. I. Regular Papers*, vol. 62, no. 6, pp. 1637–1647, 2015.

[7] G. Kaddoum and F. Gagnon, "Design of a high-data-rate differential chaos shift keying system," *IEEE Transactions on Circuits and Systems II: Express Briefs*, vol. 59, no. 7, pp. 448–452, 2012.

[8] G. Kaddoum and E. Soujeri, "NR-DCSK: a noise reduction differential chaos shift keying system," *IEEE Transactions on Circuits and Systems II: Express Briefs*, vol. 63, no. 7, pp. 648–652, 2016.

[9] G. Kaddoum, "Design and performance analysis of a multiuser OFDM based differential chaos shift keying system," *IEEE Transactions on Communications*, vol. 64, no. 1, pp. 249–260, 2016.

[10] G. Kaddoum, E. Soujeri, and Y. Nijsure, "Design of a short reference noncoherent chaos-based communication systems," *IEEE Transactions on Communications*, vol. 64, no. 2, pp. 680–689, 2016.

[11] Y. Xiao, *MIMO: Multiple Antenna Communication System*, Post & Telecom Press, Beijing, China, 1st edition, 2009.

[12] Y. Fang, J. Xu, L. Wang, and G. Chen, "Performance of MIMO relay DCSK-CD systems over nakagami fading channels," *IEEE Transactions on Circuits and Systems I: Regular Papers*, vol. 60, no. 3, pp. 757–767, 2013.

[13] L. Wang, X. Min, and G. Chen, "Performance of SIMO FM-DCSK UMB system based on chaotic pulse cluster signals," *IEEE Transactions on Circuits and Systems. I. Regular Papers*, vol. 58, no. 9, pp. 2259–2268, 2011.

[14] P. Chen, L. Wang, and F. C. M. Lau, "One analog STBC-DCSK transmission scheme not requiring channel state information," *IEEE Transactions on Circuits and Systems I: Regular Papers*, vol. 60, no. 4, pp. 1027–1037, 2013.

[15] H. Yang and G.-P. Jiang, "Reference-modulated DCSK: a novel chaotic communication scheme," *IEEE Transactions on Circuits and Systems II: Express Briefs*, vol. 60, no. 4, pp. 232–236, 2013.

[16] G. Kaddoum, E. Soujeri, C. Arcila, and K. Eshteiwi, "I-DCSK: an improved noncoherent communication system architecture," *IEEE Transactions on Circuits and Systems II: Express Briefs*, vol. 62, no. 9, pp. 901–905, 2015.

[17] S. Y. Chen, L. Wang, and G. R. Chen, "Data-aided timing synchronization for FM-DCSK UWB communication systems," *IEEE Transactions on Industrial Electronics*, vol. 57, no. 5, pp. 1538–1545, 2010.